접촉 오차 벡터를 이용한 비선형 변형체의 마찰접촉 해석

Analysis of Frictional Contact Problems of Nonlinearly Deformable Bodies by Using Contact Error Vector

이 기 수* 김 방 원**
Lee, Kisu Kim, Bang-Won

요 지

본 논문에서는 대변형 비선형 변형체의 마찰 접촉 문제의 해법을 제시하였다. 접촉 가능 점에서 접촉조건을 접촉오차 벡터를 이용하여 표시하였으며, 이러한 접촉오차 벡터를 0으로 단조 감소시키기 위하여 반복계산법을 사용하였다. 각 반복계산은 2개의 단계로 구성되어 있다 : 첫 단계에서는 이미 구해진 해의 기하학적 모양에서 얻어지는 접촉오차 벡터를 이용하여 접촉력을 수정하고, 두 번째 단계에서는 첫 단계의 접촉력을 이용하여 평형방정식을 풀어서 변위 및 접촉오차를 계산하는 것이다. 본 반복계산법에 의하여 정확한 해를 얻을 수 있음을 설명하였으며, 강소성 막 및 비선형 탄성보를 사용하여 예제계산을 수행하였다.

핵심용어 : 마찰접촉, 접촉오차 벡터, 반복계산법, 계산가속기법

Abstract

Numerical solution for frictional contact problems of nonlinearly deformable bodies having large deformation is presented. The contact conditions on the possible contact points are expressed by using the contact error vector, and the iterative scheme is used to reduce the contact error vector monotonically toward zero. At each iteration the solution consists of two steps : The first step is to revise the contact force by using the contact error vector given by the previous geometry, and the second step is to compute the displacement and the contact error vector by solving the equilibrium equation with the contact force given at the first step. Convergence of the iterative scheme to the correct solution is analyzed, and the numerical simulations are performed with a rigid-plastic membrane and a nonlinear elastic beam.

***Keywords** : frictional contact, contact error vector, iterative scheme, solution acceleration technique*

1. Introduction

Analysis of frictional contact problems of nonlinearly deformable bodies having large deformation is important in some engineering fields and various numerical techniques have been developed. Even though penalty method[1),2)], the method employing Lagrange multiplier[3),4)] and special techniques of mathematical programs and linearized techniques[5),6)] are most widely

* 정회원 · 전북대학교 기계공학과, 부교수
** 전북대학교 기계공학과 응용역학실험실, 박사과정

• 이 논문에 대한 토론을 2000년 12월 31일까지 본 학회에 보내주시면 2001년 3월호에 그 결과를 게재하겠습니다.

used for such frictional contact problems, they usually involve too complicated formulations or computational difficulties. For example the solution of the penalty method is usually sensitive to the penalty value, and the Lagrange multiplier method accompanies increased number of equations and additional considerations to solve the enlarged equations. The computational difficulties in contact problems occur mainly because the contact conditions consist of several inequality constraints. By such reasons, in,[7)~9)] the inequality constraints arising in contact problems are efficiently replaced by equality constraints by employing constraint functions which are always continuous and differentiable. Then the traditional Lagrange multiplier method and the penalty method may be easily employed to enforce the constraints, and efficient Newton Raphson iterations may be always applied to solve the global equations involving the constraints. But, the contact forces should be reasonably regularized with very small parameters in the constraint functions to strictly enforce the contact conditions.

Especially, in most of the above methods, frictional condition impose special difficulties on the solution procedure because the direction of frictional force as well as stick or slip on any contact point are not known before the solution. For example, if the condition that the frictional force should act in the opposite direction of the relative sliding is neglected, then the computed frictional force might have the same direction as that of the relative sliding. To the authors best knowledge, some of the solution techniques in the literature do not strictly impose such condition, and there is no guarantee that the correct solution is obtained by such procedure. Thus, for the frictional contact analysis of complex bodies having large deformation, it becomes very important to accurately detect the direction of frictional force as well as stick or slip on any contact point because they often cannot be reasonably guessed before the solution.

In this work it is shown that the frictional contact problems of nonlinearly deformable bodies having large deformation are solved by the iterative scheme of[10)] which was suggested for the frictional contact analysis of linear elastic bodies of small deformation. The contact error vector is defined by using the contact conditions, and all the contact conditions are satisfied by monotonically reducing the contact error vector toward zero. Thus, contact and separation, direction of frictional force, and stick or slip on any possible contact point are automatically detected by reducing the contact error vector toward zero. Also the condition that the frictional force should act in the opposite direction of the relative sliding is strictly imposed. The basic computing procedure at each iteration consists of the two steps which are similar to those of the multiplier update scheme (e.g.,[4)]). The first step is to compute the contact force by using the contact error vector determined on the geometry of the previous iteration and the second step is to compute the contact error vector after solving the global equilibrium equation with the given contact force. Moreover, even though the basic iterative scheme of this work (i.e., iterative scheme of this work with $n=1$) is similar to the multiplier update scheme (or the augmented Lagrange multiplier method), the convergence speed of the iterative scheme of this work is drastically improved by using the acceleration technique. In this work the basic computing procedures to solve the frictional contact problems are presented, the convertgence of the iterative method is analyzed, and the numerical simulations are performed to demonstrate the feasibility of the method to the problems of various constitutive equations.

2. Equations of Equilibrium and Contact Condition

In this work, two-dimensional problems of nonlinearly deformable bodies are considered and the standard finite element techniques are employed for the equation of equilibrium. Also, for the simplicity of writing, a deformable body is assumed to make contact with a rigid body. For the formulation of the equation of equilibrium, the contact force is assumed to be known before the solution (i.e., the contact force is treated as a prescribed external force in the equation of equilibrium, and its correct value is determined by the iterative scheme explained later). Then, as illustrated in Appendices A and B, by the standard finite element techniques, the equation of equilibrium of the deformable body generally takes the following form if incremental displacement is used:

$$\mathbf{A}(\Delta \mathrm{u}) = \mathbf{f} + \mathbf{T}\mathbf{p} \tag{1}$$

or the following form if total displacement is used:

$$\mathbf{A}(\mathbf{u}) = \mathbf{f} + \mathbf{T}\mathbf{p} \tag{2}$$

where $\mathbf{A}$ denotes the vector of the internal forces in the equation of equilibrium, $\mathbf{u}$ is the vector of the nodal displacements, $\Delta\mathbf{u}$ is the vector of the incremental nodal displacements, $\mathbf{f}$ is the vector of the known external forces (here, $\mathbf{f}$ is independent from the geometry of the contact surface), $\mathbf{p}$ is the vector of the unknown contact forces consisting of the normal and tangential components. Also, $\mathbf{T}$ is the matrix transforming the contact forces described in terms of the normal and tangential components to the nodal forces of FEM. As an example, if the body is modeled by using beam elements as shown in Fig. 1, $\mathbf{T}$ takes the following form:

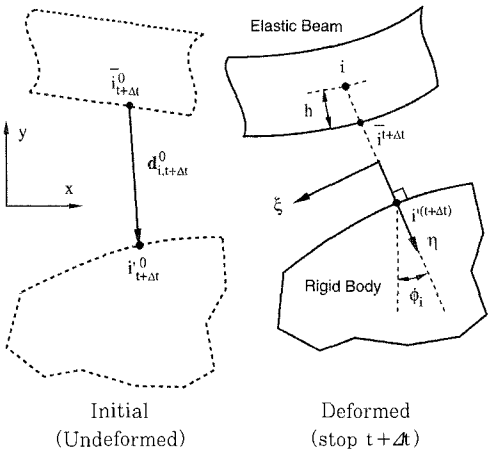

Fig. 1 Possible contact points between beam and rigid body on the configuration of step $t+\Delta t$ and on the initial configuration.

$$\mathbf{T} = \begin{bmatrix} -\cos\Phi_1 & \sin\Phi_1 & & & \\ -\sin\Phi_1 & -\cos\Phi_1 & & & \\ h & 0 & & & \\ & \cdot & & & \\ & & -\cos\Phi_i & \sin\Phi_i & \\ & & -\sin\Phi_i & -\cos\Phi_i & \\ & & h & 0 & \\ & & & \cdot & \\ & & & & \cdot \end{bmatrix} \tag{3}$$

where Φ_i is the angle denoting the normal direction at the ith contact point and h is the distance between the surface of the beam and the beam center line as shown in Fig. 1. In Fig. 1, $\bar{i}^{t+\Delta t}$ denotes the possible contact point on the beam, $i'^{(t+\Delta t)}$ denotes the contact pairing point on the rigid body, and $\bar{i}^{0}_{t+\Delta t}$ and $i'^{0}_{t+\Delta t}$ denotes the corresponding contact points on the initial configuration. A typical example of Eq. (1) is an equilibrium equation of a rigid-plastic membrane shown in Appendix A, and a typical example of Eq. (2) is an equilibrium equation of a nonlinear elastic beam shown in Appendix B, and Eqs. (1) and (2) may be solved by the Newton Raphson method if the values of $\mathbf{T}$ and $\mathbf{p}$ are given before solving them. For example, at time step $t+\Delta t$, Eq. (1)

may be solved by the following Newton Raphson iterations if the values of **T** and **p** are given before solving Eq. (1):

$$\left(\frac{\partial \mathbf{A}(\Delta \mathbf{u})}{\partial \Delta \mathbf{u}}\right)_j^{t+\Delta t} \delta \mathbf{u}_{j+1}^{t+\Delta t} = \mathbf{T}^{t+\Delta t}\mathbf{p}^{t+\Delta t} + \mathbf{f}^{t+\Delta t} - (\mathbf{A}(\Delta \mathbf{u}))_j^{t+\Delta t} \tag{4}$$

$$\Delta \mathbf{u}_{j+1}^{t+\Delta t} = \Delta \mathbf{u}_j^{t+\Delta t} + \delta \mathbf{u}_{j+1}^{t+\Delta t} \tag{5}$$

where $t+\Delta t$ denotes the time step and j denotes the iteration. Even though this work does not deal with a dynamic problem, as the frictional force and the solution of the equilibrium equation of nonlinearly deformable body generally depend on the deformation process, the time step is used to denote the loading step of the external forces. In this work, at each time step, after giving the value of contact force **p** by the iterative scheme which will be explained in the next section, Eq. (1) or (2) is solved and displacement **u** is computed. Whenever displacement **u** is computed at each iteration of each time step, the contact pairing points on the rigid body are determined by drawing the normal lines from the nodal points of a deformable body as shown in Fig. 1 (it is quite natural that the normal direction should be determined on the current configuration). Then, the normal direction, η, and the tangential direction, ξ, are determined as shown in Fig. 1, and transformation matrix **T** is computed. In Fig. 1, point i denotes the nodal point of the beam, $\bar{\mathrm{i}}^{t+\Delta t}$ denotes the possible contact point on the beam surface at time step $t+\Delta t$, and $\mathrm{i}'^{(t+\Delta t)}$ denotes the contact pairing point on the rigid body at time step $t+\Delta t$, respectively.

In this work the displacements of the possible contact points on the surface of the deformable body is denoted as $\bar{\mathbf{u}}$. For example, $\bar{\mathbf{u}}$ consists of the displacements of the nodal points on the possible contact surface if the body is modeled by isoparametric plane-stress elements, and $\bar{\mathbf{u}}$ consists of the displacements of the surface points (e.g., point $\bar{\mathrm{i}}^{t+\Delta t}$ in Fig. 1) if the body is modeled by beam elements. In Fig. 1, point $\bar{\mathrm{i}}^{0}_{t+\Delta t}$ and $\mathrm{i}'^{0}_{t+\Delta t}$ denote the initial positions of points $\bar{\mathrm{i}}^{t+\Delta t}$ and $\mathrm{i}'^{(t+\Delta t)}$ on the initial undeformed configuration, respectively. Also, in Fig. 1, $\mathbf{d}^{0}_{\mathrm{i},t+\Delta t}$ denote the initial gap between points $\bar{\mathrm{i}}^{0}_{t+\Delta t}$ and $\mathrm{i}'^{0}_{t+\Delta t}$ measured on the initial undeformed configuration. If possible contact point $\bar{\mathrm{i}}^{t+\Delta t}$ on the surface of the deformable body makes real contact with contact pairing point $\mathrm{i}'^{(t+\Delta t)}$ on the rigid body at time $t+\Delta t$, then the two points should share the same position at time step $t+\Delta t$, and thus the following relation holds:

$$\bar{\mathbf{u}}_{\mathrm{i}}^{t+\Delta t} - \mathbf{w}_{\mathrm{i}}^{t+\Delta t} - \mathbf{d}^{0}_{\mathrm{i},t+\Delta t} = 0 \tag{6}$$

where $\bar{\mathbf{u}}_{\mathrm{i}}^{t+\Delta t}$ and $\mathbf{w}_{\mathrm{i}}^{t+\Delta t}$ denote the displacements of points $\bar{\mathrm{i}}^{t+\Delta t}$ and $\mathrm{i}'^{(t+\Delta t)}$ at time step $t+\Delta t$, respectively. In this work, displacement of the rigid body, **w**, is prescribed before the solution. Even though Eq. (6) does not hold if possible contact point $\bar{\mathrm{i}}^{t+\Delta t}$ does not really contact with contact pairing point $\mathrm{i}'^{(t+\Delta t)}$ at time step $t+\Delta t$ (i.e. if the two points are separated at time step $t+\Delta t$), the tangential component of Eq. (6) is still almost valid at time step $t+\Delta t$ if point $\bar{\mathrm{i}}^{t+\Delta t}$ makes the contact at the next time step and if the external load increment between the consecutive time steps is small.

For the purpose of analysis, on the possible contact surface, vector s is defined as

$$\begin{aligned} s_{i\eta}^{t+\Delta t} &= \bar{u}_{i\eta}^{t+\Delta t} - w_{i\eta}^{t+\Delta t} - d^{0}_{i\eta,t+\Delta t} \\ s_{i\xi}^{t+\Delta t} &= \bar{u}_{i\xi}^{t+\Delta t} - w_{i\xi}^{t+\Delta t} - d^{0}_{i\xi,t} \end{aligned} \tag{7}$$

where η and ξ denote the normal and tangential directions shown in Fig. 1. Then, by using (6) of time step t and (7), if contact is made on point $\bar{i}^{t+\Delta t}$ at time step $t+\Delta t$, the following is obtained:

$$s_{i\xi}^{t+\Delta t} = \Delta \bar{u}_{i\xi}^{t+\Delta t} - \Delta w_{i\xi}^{t+\Delta t} \tag{8}$$

Thus, by definitions (6) and (7), $s_{i\eta}$ denotes the penetration and $s_{i\xi}$ denotes the incremental relative slip between contact point $\bar{i}$ and contact pairing point i' at the time step, respectively. Especially, by the above definition, the direction of $s_{i\xi}$ is the same as that of the relative tangential velocity between points $\bar{i}$ and i'.

Then, at any time step, by employing the Coulomb friction law, the contact condition on possible contact point $\bar{i}$ may be written as

$$\begin{aligned}
&p_{i\eta} \le 0 \\
&s_{i\eta} \le 0 \\
&p_{i\eta} = 0 \text{ if } s_{i\eta} < 0 \\
&s_{i\xi} = 0 \text{ if } |p_{i\xi}| < \upsilon |p_{i\eta}| \\
&s_{i\xi} = -\beta\, p_{i\xi} \text{ with some value of } \beta\,(\beta > 0) \\
&\qquad \text{if } |p_{i\xi}| = \upsilon |p_{i\eta}| > 0
\end{aligned} \tag{9}$$

where $p_{i\eta}$ and $p_{i\xi}$ denote the normal and tangential components of the contact force acting on point $\bar{i}$, and υ is the friction coefficient. In the above the third condition means that the contact pressure is zero on the separated poiont, and the fourth condition means that there is no sliding if the frictional force is smaller than the critical force of the Coulomb friction law. From the above contact condition, at any time step, for the iterative scheme of this work, contact error vector $\mathbf{v}$ is defined as

$$\begin{aligned}
v_{i\eta} &= s_{i\eta} \text{ if } p_{i\eta} < 0 \text{ or if } s_{i\eta} > 0 \\
&= 0 \text{ if } p_{i\eta} \ge 0 \text{ and } s_{i\eta} \le 0 \\
v_{i\xi} &= s_{i\xi} \text{ if } |p_{i\xi}| < \tau_i \text{ or} \\
&\quad \text{if } \{\mathrm{sign}(p_{i\xi}) = \mathrm{sign}(s_{i\xi}) \text{ and } \tau_i > 0\} \\
&= 0 \text{ if } \{|p_{i\xi}| \ge \tau_i \text{ and } \mathrm{sign}(p_{i\xi}) = -\mathrm{sign}(s_{i\xi})\} \\
&\quad \text{or if } \tau_i \le 0
\end{aligned} \tag{10}$$

where τ_i is the maximum frictional force at point $\bar{i}$ defined as

$$\tau_i = \upsilon |p_{i\eta}| \tag{11}$$

The above contact error vector is the same as that used in [10], and contact condition (9) may be written as

$$\begin{aligned}
&p_{i\eta} \le 0 \\
&|p_{i\xi}| \le \tau_i \\
&\mathbf{v} = \mathbf{0}
\end{aligned} \tag{12}$$

3. Solution Method

3.1 Iterative scheme

This work uses the iterative scheme similar to the multiplier update scheme (or augmented Lagrange multiplier method), and the computation at each iteration consists of the two major steps; the first step is to compute the frictional contact force by using the contact error vector of the previous iteration and the second step is to compute the contact error vector of the current iteration. As displacement $\mathbf{u}$ is determined by solving Eq. (1) or (2) if contact force $\mathbf{p}$ and transformation matrix T are given, contact condition (9) is automatically satisfied on the possible contact points by the solution of Eq. (1) or (2) if the correct value of contact force $\mathbf{p}$ and the correct value of transformation matrix $\mathbf{T}$ are given before solving Eq. (1) or (2). In this work, at time step $t+\Delta t$, the correct value of contact force $\mathbf{p}^{t+\Delta t}$ is determined by monotonically reducing contact

error vector $\mathbf{v}^{t+\Delta t}$ by using the following iterative scheme:

$$\begin{aligned}
\bar{\mathbf{p}}^{t+\Delta t,m} &= \mathbf{p}^{t+\Delta t,m-1} \\
&\quad - \alpha\ \mathbf{M}_n\ \mathbf{v}^{t+\Delta t,m-1}/\|\mathbf{C}'\|_\infty \\
p_{i\eta}^{t+\Delta t,m} &= \min(0,\ \bar{p}_{i\eta}^{t+\Delta t,m}) \\
p_{i\xi}^{t+\Delta t,m} &= \mathrm{sign}(\bar{p}_{i\xi}^{t+\Delta t,m})\min(|\bar{p}_{i\xi}^{t+\Delta t,m}|,\ \tau_i^{t+\Delta t}) \\
&\quad \text{if } v_{i\xi}^{t+\Delta t,m-1} = s_{i\xi}^{t+\Delta t,m-1} \\
&= \mathrm{sign}(p_{i\xi}^{t+\Delta t,m})\,\tau_i^{t+\Delta t} \\
&\quad \text{if } v_{i\xi}^{t+\Delta t,m-1} = 0 \neq s_{i\xi}^{t+\Delta t,m-1}
\end{aligned} \tag{13}$$

In the above iterative scheme, which is the same as that used in [10], m is the iteration counter, α is a constant which will be explained in the following sections, n is the acceleration index shown in Appendix C, $\mathbf{M}_n$ and $\mathbf{C}'$ are matrices shown in [10] and are also explained in Appendix C, Also, $\mathbf{s}^{t+\Delta t,m-1}$ and $\mathbf{v}^{t+\Delta t,m-1}$ denote vectors $\mathbf{s}^{t+\Delta t}$ and $\mathbf{v}^{t+\Delta t}$ computed by (7) and (10) using the solution of Eq. (1) or (2) corresponding to contact force $\mathbf{p}^{t+\Delta t,m-1}$. Even though $\tau_i^{t+\Delta t}$ in (13) should be computed as $\upsilon|p_{i\eta}^{t+\Delta t,m}|$ by (11), if any convergence problem occurs during the iterations or if the acceleration technique is employed (i.e., $n \geq 2$), $\tau_i^{t+\Delta t}$ should be approximately computed by

$$\tau_i^{t+\Delta t} = \upsilon\,|p_{i\eta}^{*}| \tag{14}$$

where $p_{i\eta}^{*}$ denotes the approximate value of $p_{i\eta}^{t+\Delta t}$ and should be kept as a constant during the iterations if the acceleration technique is employed. In the practical computation, by employing $p_{i\eta}^{t}$ determined at step t as $p_{i\eta}^{*}$, an approximate solution of step $t+\Delta t$ may be obtained by using iterative scheme (13). And a more accurate solution may be obtained if additional iterations are performed by employing $p_{i\eta}^{t+\Delta t}$ determined in the approximate solution of step $t+\Delta t$ as $p_{i\eta}^{*}$. Even though (11) is not strictly satisfied by such technique, this kind of error becomes small if the external load increment between the consecutive time steps is small.

In this work, at each iteration, the displacement is computed by solving the global equilibrium equation (1) or (2) with the contact force given by iterative scheme (13). Then, at each iteration, the positions of the possible contact pairing points on the rigid body are determined by drawing the normal lines from the nodal points of the deformable body as shown in Fig. 1, and transformation matrix $\mathbf{T}$ is computed. Finally, at each iteration, contact error vector (10) is computed by using the contact force and the displacement obtained above. Such procedure of the solution is similar to that of multiplier update scheme (e.g., [4, 11]) in the sense that only displacement is computed by solving equilibrium Eq. (1) or (2) and that the contact force is updated by (13). Also, as matrix $\mathbf{M}_n$ may be regarded to be a unit diagonal matrix if n is one, iterative scheme (13) becomes the stationary Richardson method (e.g., [12]) if n is one, $\mathbf{p}$ is taken to be $\bar{\mathbf{p}}$, $\mathbf{v}$ is taken to be s, and Eq. (1) consists of the linear equations of displacements. But it is worth to note that, even though the iterative scheme of this work is similar to the multiplier update scheme (or augmented Lagrange multiplier method), the convergence speed of the iterative scheme of this work is drastically improved by using matrix $\mathbf{M}_n$ as shown in [10].

3.2 Analysis of convergence of the iterative scheme

In this section the monotone reduction of

contact error vector (10) at time step $t+\Delta t$ by iterative scheme (13) is examined. As the present method is essentially the same as that used in,[10] only brief explanations are given here, and superscript $t+\Delta t$ is eliminated for the sake of simplicity.

By (1) or (2), (7), (13), and (14), the following conditions can be always satisfied on possible contact point $\bar{i}$ by taking a small value of α in iterative scheme (13):

$$\begin{aligned}
&\text{if } p_{i\eta}^{m-1}<0, \text{ then } \bar{p}_{i\eta}^{m}\le 0\\
&\text{if } s_{i\eta}^{m-1}<0, \text{ then } s_{i\eta}^{m}\le 0\\
&\text{if } p_{i\xi}^{m-1}>0, \text{ then } p_{i\xi}^{m}\ge 0\\
&\text{if } p_{i\xi}^{m-1}<0, \text{ then } p_{i\xi}^{m}\le 0\\
&\text{if } s_{i\xi}^{m-1}>0, \text{ then } s_{i\xi}^{m}\ge 0\\
&\text{if } s_{i\xi}^{m-1}<0, \text{ then } s_{i\xi}^{m}\le 0\\
&\text{if } |p_{i\xi}^{m-1}|<\tau_i, \text{ then } |\bar{p}_{i\xi}^{m}|\le \tau_i
\end{aligned} \tag{15}$$

where superscripts m-1 and m denote the values corresponding to contact forces $\mathbf{p}^{m-1}$ and $\mathbf{p}^{m}$, respectively. For example, $s_{i\eta}^{m}$ denotes $s_{i\eta}$ computed by (7) using the solution of Eq. (1) or (2) corresponding to contact force $\mathbf{p}^{m}$. Then, assuming a small value of α, from (13) and (15), the following is obtained:

$$\mathbf{p}^{m}-\mathbf{p}^{m-1}=-\alpha\,\mathbf{M}_n\mathbf{v}^{m-1}/\|\mathbf{C}'\|_\infty \tag{16}$$

From (7), when $\mathbf{p}^{m}-\mathbf{p}^{m-1}$ is small in iterative scheme (13), the change of $\mathbf{s}$ is related to the change of $\bar{\mathbf{u}}$ by the following:

$$\mathbf{s}^{m}-\mathbf{s}^{m-1}\approx\bar{\mathbf{u}}^{m}-\bar{\mathbf{u}}^{m-1} \tag{17}$$

When $\mathbf{p}^{m}-\mathbf{p}^{m-1}$ is small in iterative scheme (13), the corresponding variation of the displacement is also small, and the following is obtained because the work is independent of the coordinates:

$$\bar{\mathbf{u}}^{m}-\bar{\mathbf{u}}^{m-1}\approx\bar{\mathbf{T}}^{T}(\tilde{\mathbf{u}}^{m}-\tilde{\mathbf{u}}^{m-1}) \tag{18}$$

where δ denotes the small change, $\bar{\mathbf{T}}$ denotes the average value of transformation matrix $\mathbf{T}$ employed in Eq. (1) or (2) between iterations m and m-1, and $\tilde{\mathbf{u}}$ denotes the nodal displacements associated with the possible contact surface (i.e., vector $\tilde{\mathbf{u}}$ is a part of vector $\mathbf{u}$). From (4) (or from the equivalent equation corresponding to (2)), when contact force $\mathbf{p}$ changes by iterative scheme (13), the following relation is obtained:

$$\tilde{\mathbf{u}}^{m}-\tilde{\mathbf{u}}^{m-1}\approx\bar{\mathbf{K}}^{-1}\bar{\mathbf{T}}(\mathbf{p}^{m}-\mathbf{p}^{m-1}) \tag{19}$$

where $\bar{\mathbf{K}}^{-1}$ is a submatrix of the inverse of the tangential stiffness matrix of equilibrium equation (1) or (2). Then, by assuming a small value of α in iterative scheme (13), from (17), (18) and (19), the following is obtained:

$$\mathbf{s}^{m}-\mathbf{s}^{m-1}\approx\mathbf{C}(\mathbf{p}^{m}-\mathbf{p}^{m-1}) \tag{20}$$

where $\mathbf{C}$ is the matrix defined as

$$\mathbf{C}\approx\bar{\mathbf{T}}^{T}\bar{\mathbf{K}}^{-1}\bar{\mathbf{T}} \tag{21}$$

As the above relations (15)~(21) are obtained with the assumption of small change in contact force $\mathbf{p}$, they are valid if the value of $\alpha\,\mathbf{v}^{t+\Delta t,m-1}$ is small in iterative scheme (13). Thus, in practice, matrix $\mathbf{C}$ may be regarded as symmetric and positive definite because α may be reduced to a smaller value whenever required in the computation as shown in Fig. 2 (here, the tangential stiffness matrix of the equilibrium equation is assumed to be positive definite because this assumption is also required for the convergence of Newton Raphson iterations of Eqs. (1) and (2) even without contact condition).

Even though matrix **C** defined above changes as the deformation proceeds nonlinearly, the change of matrix **C** between the consecutive iterations is not large when contact error vector is small in iterative scheme (13), and thus the acceleration technique of [10] can be applied for an efficient computation in such iteration steps.

Multiplying the both sides of (20) by $\mathbf{E}(\mathbf{v}^{m-1})$ defined by (C.2), and using (16) and matrix $\mathbf{C}'$ defined by (C.1), the following is obtained:

$$\mathbf{E}(\mathbf{v}^{m-1})\,\mathbf{s}^m - \mathbf{v}^{m-1} \approx -\alpha\,\mathbf{C}'\,\mathbf{M}_n\,\mathbf{v}^{m-1}/\|\mathbf{C}'\|_\infty \qquad (22)$$

By using matrix $\mathbf{C}_n$ defined by (C.3) and using (C.8), equation (22) may be rearranged as

$$\mathbf{E}(\mathbf{v}^{m-1})\,\mathbf{s}^m \approx (\mathbf{I} - \alpha\,\mathbf{C}_n)\,\mathbf{v}^{m-1} \qquad (23)$$

As matrix **C** is positive definite, after excluding the rows and columns whose corresponding components of vector v are identically defined as zeroes by (10), matrix $\mathbf{C}_n$ becomes positive definite. When (15) is satisfied by using small α in iterative scheme (13), from (10), the component of $\mathbf{v}^m$ is zero as long as the corresponding component of $\mathbf{v}^{m-1}$ is zero. Thus, using (C.2), the following is obtained:

$$\|\mathbf{v}^m\|_2 = \|\mathbf{E}(\mathbf{v}^m)\mathbf{s}^m\|_2 \le \|\mathbf{E}(\mathbf{v}^{m-1})\mathbf{s}^m\|_2 \qquad (24)$$

From (23) and (24), the inequality

$$\|\mathbf{v}^m\|_2 < \|\mathbf{v}^{m-1}\|_2 \qquad (25)$$

is obtained if the following condition is satisfied:

$$0 < \alpha < \frac{2}{(\Lambda_n)_{max}} \qquad (26)$$

where $(\Lambda_n)_{max}$ is the maximum eigenvalue of matrix $\mathbf{C}_n$. Thus contact error (10) can be monotonically reduced toward zero by iterative scheme (13) and contact condition (12) can be satisfied by iterative scheme (13). Also, it is worth to note that, as the contact error vector is monotonically reduced toward zero by the iterative scheme, the correct contact pairing points and the correct transformation matrix **T** are computed by drawing the normal lines on the possible contact surface as shown in Fig. 1 at each iteration.

3.3 Acceleration technique

Iteration matrix $(\mathbf{I} - \alpha\,\mathbf{C}_n)$ in (23) has the minimum spectral radius

$$\rho(\mathbf{I} - \alpha\,\mathbf{C}_n) = \frac{(\Lambda_n)_{max} - (\Lambda_n)_{min}}{(\Lambda_n)_{max} + (\Lambda_n)_{min}} \qquad (27)$$

when the value of α is given by

$$\alpha = \frac{2}{(\Lambda_n)_{max} + (\Lambda_n)_{min}} \qquad (28)$$

where Λ_n denotes the eigenvalue of matrix $\mathbf{C}_n$. As $(\Lambda_n)_{max}/(\Lambda_n)_{min}$ decreases rapidly toward 1 as the value of n increases, the convergence speed of iteration scheme (13) may be improved as the value of n increases.[10]

3.4 Computer implementation

Even though α in iterative scheme (13) should be very small in some steps if condition (15) should be strictly satisfied, in the practical computation, condition (15) need not be satisfied as long as contact error vector is reduced by iterative scheme (13). Thus, for the computation, by using (28), the optimum value of α in iterative scheme (13) is given by

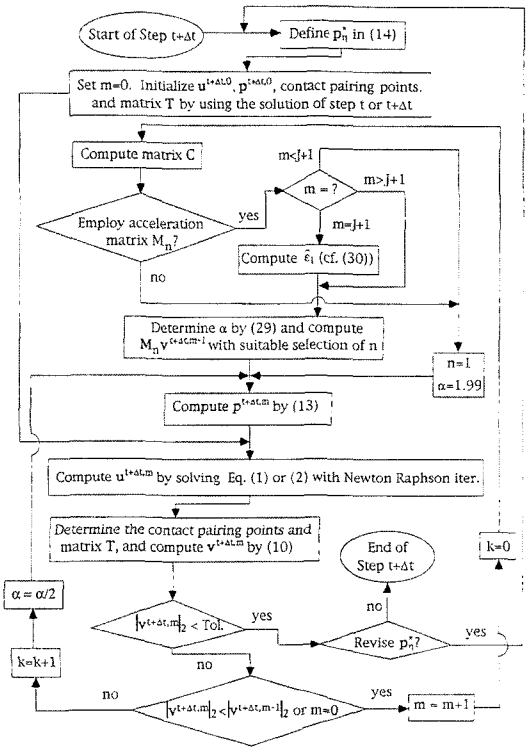

Fig. 2 Computing procedure at time step $t+\Delta t$

$$\alpha = \frac{2}{\omega_n + \varepsilon_n} \tag{29}$$

where ω_n and ε_n are computed by the definitions in Appendix C (but the mth iteration should be repeated with a reduced value of α whenever $\|\mathbf{v}^m\|_2$ does not become smaller than $\|\mathbf{v}^{m-1}\|_2$ as shown in Fig. 2). For an efficient computation, $\bar{\varepsilon}_1$, in (C.6) should be close to the minimum positive eigenvalue of matrix $\mathbf{C}_1$. In this work, when $\bar{\varepsilon}_1$ is required to be computed, n and α are set to be 1 and 1.99, respectively, in iterative scheme (13), and $\bar{\varepsilon}_1$ is estimated by the initial iterations between m=I and m=J (e.g., I=5, J=2) by the following way:

$$\bar{\varepsilon}_1 = \min_{I \le m \le J} \frac{1}{\alpha}\left(1 - \frac{\|\mathbf{v}^m\|_2}{\|\mathbf{v}^{m-1}\|_2}\right) \tag{30}$$

In the above the initial (I-2) iterations are not considered in estimating $\bar{\varepsilon}_1$ because the solutions obtained in the initial few iterations may be different from the correct solution by relatively large amount. The values of I and J are not critical in computing, and they may be selected by the user without any difficulty (e.g., I=3, J=10).

The major tasks of this work are to compute contact force **p** and displacement **u** at each time step by solving equilibrium equation (1) or (2) with contact condition (9), and the computing procedure at time step $t+\Delta t$ is shown in Fig. 2.

4. Numerical Example

4.1 Sheet stretching involving large plastic deformation

In this example a sheet stretching problem of metal forming is solved. The sheet is assumed to be rigid-plastic membrane with the equations of equilibrium shown in Appendix A, and the punch and die are treated as rigid bodies. The initial shape of the model is shown in Fig. 3, and the punch moves downward for the sheet stretching operation. This problem, which is shown in [13], is solved here with the same data used in [13]. The data of the geometries of the punch and die shown in Fig. 3 are given as R_p=50.8mm, R_d=6.35mm, and $C_d = R_0$=59.18mm, respectively. Also, the thickness of the sheet is 1mm, the both ends of the sheet are fixed, and the plane strain condition is assumed along the width direction. The values of the parameters of the rigid-plastic equations shown in Appendix A are given as r=1.0, M=2.0, H=589MPa, a_0=0.0001, and n=0.216, respectively. For the computation, the right half of the sheet was divided into 30 elements, friction coefficient was assumed

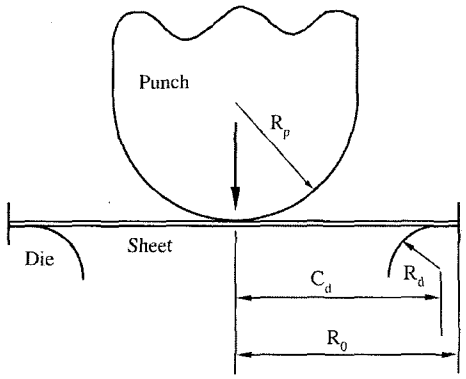

Fig. 3 Punch, die, and sheet metal before forming operation

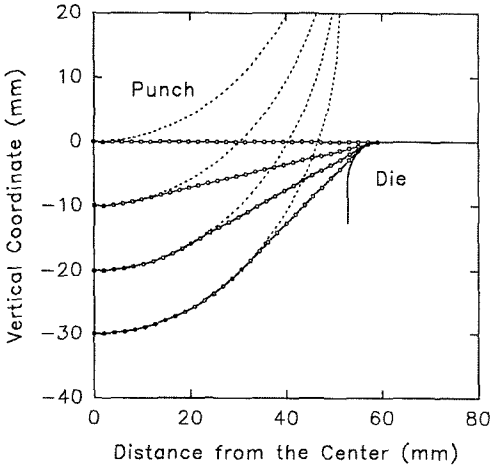

Fig. 4 Deformed sheet geometries at various punch heights

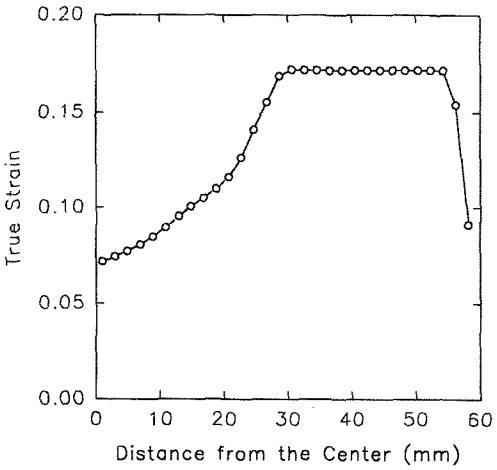

Fig. 5 True strain distribution at punch height 30mm

to be 0.15, and the punch was assumed to move downward by 1mm at each time step.

As explained in the previous section, contact condition (9) is enforced by using contact error vector (10), and Eq. (1) is solved by the Newton Raphson method with contact force **p** given by (13). The deformed geometries of the sheet at various punch positions are shown in Fig. 4 which indicates that the contact conditions are properly enforced. The computed distribution of strain in the membrane when the punch travels 30mm is shown in Fig. 5 which agrees well with that of [13].

4.2 Elastic beam bent around a rigid circular cylinder

In this example an elastic beam is bent around a rigid cylinder as shown in Fig. 6. This model is the same as that solved in [5]. Young's modulus of the beam is 210,000kg/cm^2, Poisson's ratio of the beam is 0.3, force F is 500kg, and the friction coefficient is 0.2, respectively. As the equilibrium equations of the beam subjected to large deformation are generally very complicated, relatively simplified equilibrium equations in [14] are employed here. The internal forces and the corresponding tangential stiffness matrix of the Timoshenko beam of moderately large deformation shown in [14] are summarized in Appendix B.

The right half of the beam was modeled by 40 beam elements using the three-node shape functions as shown in Appendix B, and contact forces were assumed to exist on the both end-nodes of each element. The vertical load F acting on the right upper corner of the beam was applied in 20 equal increments.

The computed contact pressure distributions are shown in Figs. 7 and 8 with the deformed shape of the beam. Here, the stress was computed by dividing the contact force by the

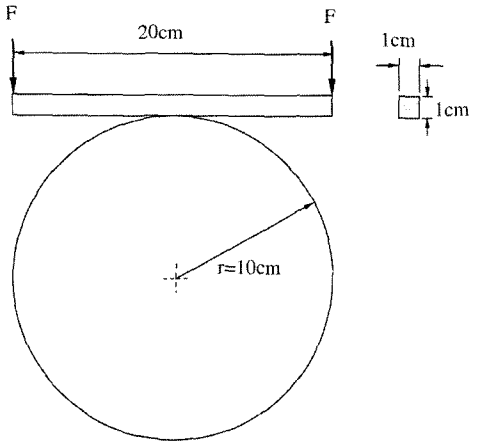

Fig. 6 Initial shape of the beam on a rigid cylinder

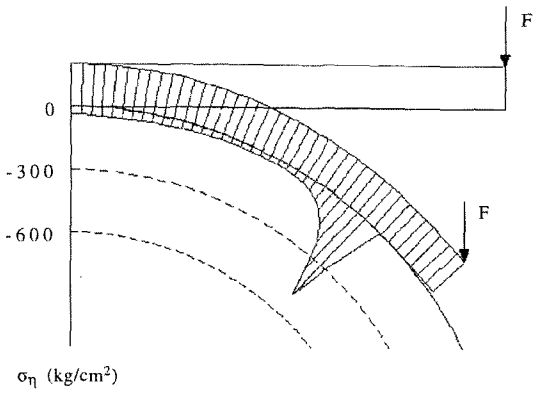

Fig. 7 Normal contact stress on the deformed shape of the beam

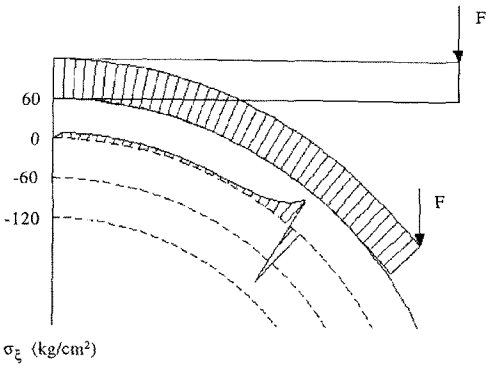

Fig. 8 Frictional contact stress on the deformed shape of the beam

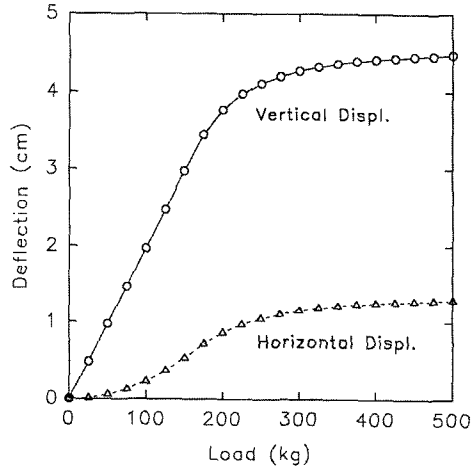

Fig. 9 Load-end deflection relations of the beam

corresponding area of the beam. Even though the normal contact stress in Fig. 7 is similar to that of, [5] the fictional stress in Fig. 8 is different from that of [5] (especially, the fictional stress changes its direction). Such difference seems to occur because the present work employs the incremental friction law explained in section 2. In the present solution, when load F is increased, the left beam elements in Fig. 8 which have maintained contact with the cylinder from the previous time steps move incrementally to the right because tension develops in these elements due to the rightward frictional force acting on the new contact surface on the right of the beam which move to the left by bending deformation (note that almost no additional bending deformation occurs on the left elements which have maintained contact with the cylinder from the previous time steps), As the frictional force takes the opposite direction of the incremental relative slip, the leftward frictional forces develop on the left beam elements shown in Fig. 8. And the displacements of the end point of the beam are shown in Fig. 9. The slight difference between Fig. 9 and the corresponding solution of [5] seems to occur because the present work employs the relatively simple equilibrium equations of the beam.

5. Concluding Remarks

Frictional contact problems of nonlinearly deformable bodies have been solved by using the iterative scheme and the contact error vector. At each iteration the contact force has been computed by using the contact error vector, and the global equilibrium equation has been solved with the given contact force. Contact conditions have been enforced by reducing the contact error vector toward zero, and thus the correct contact points and the correct directions of the frictional forces have been automatically computed without any previous guess before the solution. The convergence of the iterative scheme has been analyzed, and the applicability of the method has been demonstrated by the numerical experiments using rigid-plastic membrane and nonlinear elastic beam.

References

1. Oden, J.T. and Pires, E. B., "Algorithms and numerical results for finite element approximations of contact problems with non-classical frictional laws", *Computers and Structures*, 19, 1984, pp.137~147
2. Cheng, J.-H. and Kikuchi, N.,"An analysis of metal forming processes using large deformation elastic-plastic formulations.", *Computer Methods in Applied Mechanics and Engineering*, 49, 1985, pp.71~108
3. Chaudhary, A. and Bathe, K.J., "A solution method for static and dynamic analysis of three-dimensional contact problems with friction", *Computers and Structures*, 24, 1986, pp.855~873
4. Laursen, T.A. and Simo, J.C., "Algorithmic symmetrization of Coulomb frictional problems using augmented Lagrangians", *Computer Methods in Applied Mechanics and Engineering*, 108, 1993, pp.133~146
5. Sun, S.M., Natori, M.C. and Park, K.C., "A computational procedure for flexible beams with frictional contact constraints", *International Journal for Numerical Methods in Engineering*, 36, 1993, pp.3781~3800
6. Klarbring, A. and Bjorkman, G., "Solution of large displacement contact problems with friction using Newton's method for generalized equations", *International Journal for Numerical Methods in Engineering*, 34, 1992, pp. 249~269
7. Bathe, K.J., *Finite Element Procedures*, Prentice Hall, Englewood Cliffs, NJ, 1996, pp. 622-628
8. Eterovic, A.L. and Bathe, K.J., "On the treatment of inequality constraints arising form contact conditions in finite element analysis", *Computers and Structures*, 40, 1991, pp.203~209
9. Bathe, K.J. and P.A. Bouzinov, "On the constraint function method for contact problems", *Computers and Structures*, 64, 1997, pp. 1069~1085
10. Lee, K., "An efficient solution method for frictional contact problems", *Computers and Structures*, 32, 1989, pp.1~11
11. Luenberger, D.G., *Linear and Nonlinear Programming*, Addison-Wesley, Reading, Massachusetts, 1984, pp.436~437
12. Young, D.M., *Iterative Solution of Large Linear Systems*, Academic Press, New York, 1971, pp.74
13. Choudhary, S. and Lee, J.K., "Dynamic plane strain finite element simulation of industrial sheet-metal forming processes", *International Journal of Mechanical Science, 36, 1994, pp.189~207*
14. Crisfield, M.A., *Non-linear Finite Element Analysis of Solids and Structures*, Vol. 1,

John Wiley and Sons, Chichester, 1991, pp.208~209
15. Germain, Y., Chung, K. and Wagoner, R.H., "A rigid-viscoplastic finite element program for sheet metal forming analysis", *International Journal of Mechanical Science*, 31, 1989, pp.1~24

(접수일자 : 1999. 8. 30)

Appendix A : Equations of Equilibrium of a Rigid-Plastic Membrane

In the numerical example of this work the rigid-plastic equations of membrane used for sheet forming analysis in [15] are employed, and are briefly summarized here. Following the procedures of [15] the hardening law, effective stress $\bar{\sigma}$, and incremental effective strain $\Delta\bar{\varepsilon}$ are expressed as

$$\bar{\sigma}=H(\bar{\varepsilon}+a_0)^n \tag{A.1}$$

$$\bar{\sigma}=[2(1+r)]^{-1/M} \times[|\sigma_1+\sigma_2|^M+(1+2r)|\sigma_1-\sigma_2|^M]^{1/M} \tag{A.2}$$

$$\Delta\bar{\varepsilon}=0.5[2(1+r)]^{1/M}[|\Delta\bar{\varepsilon_1}+\Delta\bar{\varepsilon_2}|^{M/(M-1)} + [1+2r]^{-1/(M+1)}|\Delta\bar{\varepsilon_1}-\Delta\bar{\varepsilon_2}|^{M/(M-1)}]^{(M-1)/M} \tag{A.3}$$

where r and M are the normal anisotropy parameter and the index describing the shape of the yield surface, respectively. And incremental effective strain $\Delta\bar{\varepsilon}$ is computed by

$$\Delta\bar{\varepsilon}=0.5[2(1+r)]^{1/M}[|\ln(\lambda_1\lambda_2)|^{M/(M-1)} + [1+2r]^{-1/(M+1)}\left|\ln(\frac{\lambda_1}{\lambda_2})\right|^{M/(M-1)}]^{(M-1)/M} \tag{A.4}$$

where λ_1 and λ_2 are principal stretch ratios of the membrane. And the equation of equilibrium on nodal point k is obtained as

$$\int\bar{\sigma}\frac{\partial\Delta\bar{\varepsilon}}{\partial\Delta\mathbf{u}_k}dv=\mathbf{q}_k \tag{A.5}$$

where $\Delta\mathbf{u}_k$ and $\mathbf{q}_k$ are the incremental displacement and the force vectors on nodal point k, and the integration is performed on the related volume. When the external force consists of the prescribed external force and the unknown contact force, by following the procedures of [15], Eq. (A.5) may be written in the form of Eq. (1).

Appendix B : Equations of Equilibrium of an Elastic Beam Having Moderately Large Displacement

The equilibrium equations of Timoshenko beam of moderately large-deflection shown in [14], which are employed in the numerical example of this work, are summarized here. From a typical beam element whose axial and transversal directions are denoted by x and z, respectively, normal strain ε_x is assumed to be

$$\varepsilon_x=\frac{du}{dx}+\frac{1}{2}\left(\frac{dw}{dx}\right)^2-z\frac{d^2w}{dx^2} \tag{B.1}$$

where u and w are the axial and transversal displacements of the beam center line. In each element, displacements of the beam center line u and w and rotation of the cross-section θ are interpolated by the following:

$$u=\mathbf{h}^T\mathbf{u},\quad w=\mathbf{h}^T\mathbf{w},\quad \theta=\mathbf{h}^T\boldsymbol{\theta} \tag{B.2}$$

where

$$\mathbf{h}^T=\frac{1}{2}\{1-\varphi,1+\varphi,2(1-\varphi^2)\}$$
$$\mathbf{u}^T=(u_1,u_2,\Delta u_q),\quad \mathbf{w}^T=(w_1,w_2,\Delta w_q),$$
$$\boldsymbol{\theta}^T=(\theta_1,\theta_2,\theta_q) \tag{B.3}$$

In the above $\mathbf{u}$, $\mathbf{w}$, and $\boldsymbol{\theta}$ denote the nodal values and φ denotes the coordinate in an element having three nodes. And axial force N, shear force Q, and bending moment M are given as

$$N = EA\overline{\varepsilon} = EA\left\{\mathbf{b}^T\mathbf{u} + \frac{1}{2}(\mathbf{b}^T\mathbf{w})^2\right\}$$
$$Q = k'GA(\mathbf{b}^T\mathbf{w} + \mathbf{h}^T\boldsymbol{\theta})$$
$$M = EI\mathbf{b}^T\boldsymbol{\theta} \qquad (B.4)$$

where

$$\mathbf{b}^T = \frac{1}{L}(-1,\ 1,\ -4\varphi) \qquad (B.5)$$

After applying the principle of virtual work, the corresponding tangential stiffness matrix is given as

$$\mathbf{K} = \begin{bmatrix} \mathbf{K}_{uu} & \mathbf{K}_{uw} & 0 \\ \mathbf{K}_{wu} & \mathbf{K}_{ww} & \mathbf{K}_{w\theta} \\ 0 & \mathbf{K}_{\theta w} & \mathbf{K}_{\theta\theta} \end{bmatrix} \qquad (B.6)$$

where

$$\mathbf{K}_{uu} = \int EA\mathbf{b}\mathbf{b}^T dx$$
$$\mathbf{K}_{uw} = \int EA(\mathbf{b}^T\mathbf{w})\mathbf{b}\mathbf{b}^T dx$$
$$\mathbf{K}_{ww} = \int \{EA(\mathbf{b}^T\mathbf{w})^2\mathbf{b}\mathbf{b}^T + GA\mathbf{b}\mathbf{b}^T + N\mathbf{b}\mathbf{b}^T\} dx$$
$$\mathbf{K}_{w\theta} = \int GA\mathbf{b}\mathbf{h}^T dx$$
$$\mathbf{K}_{\theta\theta} = \int (EI\mathbf{b}\mathbf{b}^T + GA\mathbf{h}\mathbf{h}^T) dx \qquad (B.7)$$

Appendix C : Matrices for Solution Acceleration

For efficient computations of the iterative scheme, the acceleration technique shown in [10] is employed in this work, and only the necessary matrices are outlined here. For the solution acceleration, from matrix $\mathbf{C}$ defined by (21), matrix $\mathbf{C}'$ is defined as

$$\mathbf{C}' = \mathbf{E}(\mathbf{v}^{m-1})\mathbf{C}\mathbf{E}(\mathbf{v}^{m-1}) \qquad (C.1)$$

where $\mathbf{E}(\mathbf{v}^{m-1})$ is a diagonal matrix defined as

$$\mathbf{E}(\mathbf{v}^{m-1})_{ii} = 1 \text{ if } v_i^{m-1} \text{ is not identically defined as zero}$$
$$= 0 \text{ if } v_i^{m-1} \text{ is identically defined as zero} \qquad (C.2)$$

In the above, $\mathbf{v}^{m-1}$ denotes the contact error vector employed in (13), and matrix $\mathbf{C}$ is symmetric and positive definite. From matrix $\mathbf{C}'$, a series of matrices, $\mathbf{C}_n$, are defined as

$$\mathbf{C}_n = \mathbf{C}'/\|\mathbf{C}'\|_\infty \quad \text{if} \quad n=1$$
$$= \mathbf{C}_{n-1}(b_n\mathbf{E} - \mathbf{C}_{n-1}) \quad \text{if} \quad n \geq 2 \qquad (C.3)$$

where

$$b_n = \varepsilon_{n-1} + \omega_{n-1} \quad (n \geq 2) \qquad (C.4)$$

$$\omega_n = 1 \quad \text{if} \quad n=1$$
$$= (b_n)^2/4 \quad \text{if} \quad n \geq 2 \qquad (C.5)$$

$$\varepsilon_n = \overline{\varepsilon}_1 \quad \text{if} \quad n=1$$
$$= \varepsilon_{n-1}\omega_{n-1} \quad \text{if} \quad n \geq 2 \qquad (C.6)$$

In the above, n is an integer number and $\overline{\varepsilon}_1$ is the assumed minimum positive eigenvalue of matrix $\mathbf{C}_1$. And matrix $\mathbf{M}_n$ is defined as

$$\mathbf{M}_n = \mathbf{E} \quad \text{if} \quad n=1$$
$$= (b_n\mathbf{E} - \mathbf{C}_{n-1})\mathbf{M}_{n-1} \quad \text{if} \quad n \geq 2 \qquad (C.7)$$